Triboelectric Nanogenerator

Subjects: Engineering, Ocean
Contributor: Liang Xu

First proposed by Wang in 2012, the triboelectric nanogenerator (TENG, also called Wang generator) derived from Maxwell's displacement current shows great prospect as a new technology to convert mechanical energy into electricity, based on the triboelectrification effect and electrostatic induction. TENGs present superiorities including light weight, cost-effectiveness, easy fabrication, and versatile material choices. The concept of harvesting blue energy using the TENG and its network was first brought out in 2014. As a new form of blue energy harvester, the TENG surpasses the EMG in that it intrinsically displays higher effectiveness under low frequency, owing to the unique feature of its output characteristics. Moreover, adopting the distributed architecture of light-weighted TENG networks can make it more suitable for collecting wave energy of high entropy compared with EMGs, which are oversized in volume and mass.

Keywords: triboelectric nanogenerator ; network ; blue energy ; wave energy ; energy harvesting

1. Introduction

Covering over 70% of the earth's surface, ocean plays a crucial role for lives on the planet and can be regarded as an enormous source of blue energy, whose exploitation is greatly beneficial for dealing with energy challenges for human beings [1][2][3]. With extreme climate conditions taking place more frequently nowadays, the world feels the urge to take immediate action to alleviate climate deterioration caused by global warming [4][5][6]. Carbon neutrality is thus put forward as a goal to reach balance between emitting and absorbing carbon in the atmosphere [7]. One of the most effective methods is to develop and expand the use of clean energy that generates power without carbon emission, such as the enormous blue energy [8]. Meanwhile, with the increasing activities in ocean, equipment deployed in the far ocean is facing problems regarding an in situ and sustainable power supply, where blue energy is an ideal source for developing new power solutions for such applications, allowing self-powered marine systems and platforms, though the harvesting scale can be much smaller [9][10][11].

The ocean blue energy is typically in five forms: wave energy, tidal energy, current energy, thermal energy, and osmotic energy, among which the wave energy is promising for its wide distribution, easy accessibility, and large reserves. The wave energy around the coastline is estimated to be more than 2 TW (1 TW = 10 12 W) globally [12]. However, the present development of wave energy harvesting is challenged by its feature as a type of high-entropy energy, which refers to the chaotic, irregular waves with multiple amplitudes and constantly changing directions that are randomly distributed in the sea [13][14]. Most significantly, wave energy is typically distributed in a low-frequency regime, yet the most common and classic method of blue energy harvesting at status quo, the electromagnetic generator (EMG), performs rather poorly in low-frequency energy harvesting, which relies on propellers or other complex mechanical structures to drive bulky and heavy magnets and metal coils in order to transform mechanical energy into electricity [8]. Thus, it usually has high cost and low reliability.

2. TENG Systems for Blue Energy Harvesting

2.1. Fundamental Working Modes of TENGs

TENGs generate electricity by the coupling of triboelectrification and electrostatic induction, which are classified into the four fundamental working modes [15]: vertical contact-separation mode, lateral sliding mode, single-electrode mode, and freestanding triboelectric-layer mode (**Figure 1**b–e).

As shown in **Figure 1**b, in vertical contact-separation mode, the two dielectric surfaces are oppositely charged after physical contact due to triboelectrification. When the two surfaces are vertically separated with a gap in between, a potential drop is produced between the two electrodes attached to the backsides of the two dielectric layers due to the separation of positive and negative static charges, which drives current to flow between the electrically connected electrodes to balance the electrostatic field. When the gap vanishes, the potential drop due to static charges exists no more and so the induced free charges flow backwards. In this way, an alternate current (AC) output is generated in the external circuit under periodic contact and separation movement of the TENG [16].

For the lateral sliding mode shown in **Figure 1**c, the two dielectric surfaces are charged through triboelectrification during initial sliding motion. Under the full alignment of the two surfaces, no potential difference by static charges is created across the electrodes, since surface static charges of opposite signs completely compensate each other. When a relative displacement paralleled to the interface is introduced under lateral sliding, the mismatched area of the dielectric layers leads to bare static charges and so a potential difference appears between electrodes. The sliding back and forth of the TENG hence results in periodical changes of potential that drive free electrons to flow between the electrodes [17].

In single-electrode mode TENG (**Figure 1**d), the moving dielectric layer no longer has to be bound to electrodes or electrically connected by wires. The only electrode essential to the mode is one electrically connected to the ground, which can be regarded as another electrode. The surface of the dielectric layer is first charged under full contact with the electrode. When they start to move apart from each other, the induced charges in the electrode decrease in order to balance the electric potential, through charge exchange with the ground. Then, when the dielectric layer moves back to contact again, electrons flow in the opposite direction to re-establish an electrostatic equilibrium until the two surfaces fully overlap. Although charge transfer is not effective as a result of electrostatic screening effect, the triboelectric layer can move freely without any restrains [18].

The freestanding triboelectric-layer mode TENG can also work with the moving dielectric layer disconnected to electrodes, yet without any screening effect (**Figure 1**e). When the dielectric layer charged by triboelectrification approaches a pair of electrodes asymmetrically, a potential difference is induced across the two electrodes, causing electrons to flow between them to balance the local potential distribution. Under the back-and-forth movement of the dielectric layer, electrons oscillate across the paired electrodes, generating an AC current output [19].

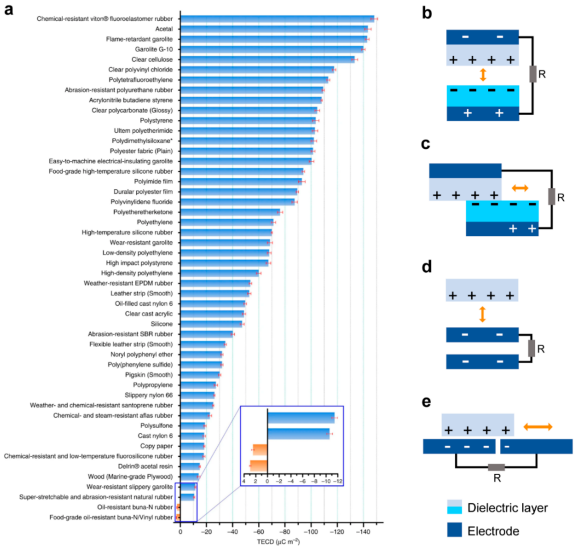

Figure 1. Triboelectric series and four fundamental working modes of TENGs. (**a**) Quantified triboelectric series. Reprinted with permission from ref. [34], Copyright 2019, Springer Nature. (**b**) Vertical contact-separation mode. (**c**) Lateral sliding mode. (**d**) Single-electrode mode. (**e**) Freestanding triboelectric-layer mode.

2.2. TENG Systems for Harvesting Blue Energy

For effectively harvesting distributed wave energy, the TENG is conceived to be organized in networks, which can have hierarchical structure of modules [20]. The network structure also enables the device to be applied in different scales of harvesting, ranging from self-powered systems to large-scale clean energy (**Figure 2**a). In the development of TENGs for blue energy, efforts are mainly focusing on four aspects: TENG unit design, networking strategy, power management, and application system (**Figure 2**b). The primary and most significant part is the fundamental design of the TENG unit, which relies on continuous improvements focusing on the structure, principle, and material to enhance its energy harvesting performance and to meet demands raised by various ocean environments, both on the water surface and beneath it. Networking strategy is then adopted to add outputs of single TENG units and expand them in a reliable way. It decides the connection pattern of massive TENG units and the coupling effect between TENG units, which could further enhance the performance. Before finally supplying electricity power to the application system, power management is required to manipulate the TENG output for a better match with appliances and improve the power efficiency with circuit approaches. This review mainly emphasizes methods to advance the design of TENG units, which is the most challenging part, and networking strategy and power management are also discussed.

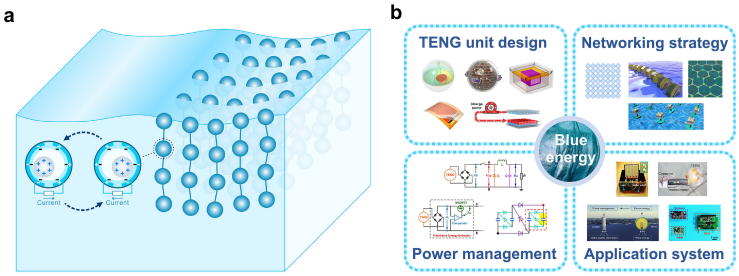

Figure 2. Schematics of blue energy harvesting based on TENGs. (**a**) Schematic diagram of the TENG network for harvesting wave energy. Reprinted with permission from ref. [21], Copyright 2021, IOP publishing, Ltd. (**b**) Schematic diagram of major aspects for blue energy harvesting based on TENGs, including TENG unit design, networking strategy, power management, and application system. Reprinted with permission from ref. [22], Copyright 2019, Elsevier. Reprinted with permission from ref. [23], Copyright 2019, Elsevier. Reprinted with permission from ref. [24], Copyright 2017, Elsevier. Reprinted with permission from ref. [25], Copyright 2015, American Chemical Society. Reprinted with permission from ref. [26], Copyright 2018, Elsevier. Reprinted with permission from ref. [27], Copyright 2019, Elsevier. Reprinted with permission from ref. [28], Copyright 2018, Elsevier. Reprinted with permission from ref. [29], Copyright 2020, Elsevier. Reprinted with permission from ref. [30], Copyright 2017, Elsevier. Reprinted with permission from ref. [31], Copyright 2020, Springer Nature. Reprinted with permission from ref. [32], Copyright 2014, American Chemical Society. Reprinted with permission from ref. [33], Copyright 2020, Springer Nature. Reprinted with permission from ref. [11], Copyright 2019, Elsevier. Reprinted with permission from ref. [20], Copyright 2017, Springer Nature.

3. Summary and Perspectives

Different kinds of structure designs of TENG unit, including including rolling ball structure, multilayer structure, grating structure, pendulum structure, mass-spring structure, spacing structure, water-solid contact structure, and charge pumping strategy, are born with advantages to cater to specific needs, including the naturally low frequency of rolling ball structure to match with slow wave agitations, the superior output density of multilayer and grating structures, the high sensitivity and elongated operation time under mechanical excitations to improve the energy conversion efficiency through pendulum and mass-spring structures, and the outstanding robustness and durability by spacing structure. Principle innovation such as charge pumping is significant as it can bring large promotion to the system. Networking strategy and power management are also briefly discussed. As a promising clean energy technology, blue energy harvesting based on TENGs is expected to make great contributions for achieving carbon neutrality and developing self-powered marine systems. Revealed as a type of mechanical energy harvester more suitable for low-frequency excitations, the key to the commercialization of TENGs lies in the combination of high power density and robustness. The following aspects are suggested to be focused upon in future investigations:

(1) The design of TENG units is still quite crucial for further enhancing the power density, especially in a real ocean environment, which has much more complex wave conditions than in the lab, and the design of the device can be further validated and optimized based on current devices [34]. A detailed comparison on typical devices is shown in **Table 1**. In general, devices based on multilayer structure and grating structure intrinsically output with greater power density. Making the components soft can expand contact area, which enhances triboelectrification. Mechanism innovations regarding charge pumping strategy achieve ultrahigh charge density. Rolling ball, pendulum, and mass-spring structures can make blue energy harvesting more adaptive to changing directions and broad frequency of waves, with better durability. To reach higher output of TENGs from the material aspect, polymers can be improved in dielectric permittivity, electrostatic breakdown strength, stability, contact status, and mechanical robustness, through surface morphology and molecular functionalization as well as bulk composition modification [35].

Table 1. Summary of typical TENG units.

Device	Feature	Typical Output				Dimension Per Unit	Material	Mode	Year	Note
		Q_{sc}	I_{sc}	Power	Power Density					
rolling-structured TENG [36] (RF-TENG)	rolling	24 nC (wave, 1.43 Hz)	1.2 μA (wave, 1.43 Hz)			sphere diameter 6 cm	Nylon, Al, Kapton	freestanding	2015	low friction

Device	Feature	Typical Output				Dimension Per Unit	Material	Mode	Year	Note
		Q_{sc}	I_{sc}	Power	Power Density					
ball-shell-structured TENG [37] (BS-TENG)	rolling	72.6 nC (motor)	1.8 μA (motor, 3 Hz)	peak: 1.28 mW (motor, 5 Hz) average: 0.31 mW (motor, 5 Hz)	peak: 7.13 W m^{-3} (motor, 5 Hz) average: 1.73 W m^{-3} (motor, 5 Hz)	sphere diameter 7 cm	silicon rubber, POM, Ag-Cu	freestanding	2018	low dampin force
3D electrode TENG [23]	rolling, multilayer	0.52 μC (motor)	5 μA (motor, 2 Hz)	peak: 8.75mW (motor, 1.67 Hz) average: 2.33 mW (motor, 1.67 Hz)	peak: 32.6 W m^{-3} (motor, 1.67 Hz) average: 8.69 W m^{-3} (motor, 1.67 Hz) 2.05 W m^{-3} (wave)	sphere diameter 8 cm	FEP, Cu	freestanding	2019	enhanced contact area
air-driven membrane structure TENG [24]	multilayer, mass-spring	15 μC (rectified, motor)	187 μA (motor) 1.77 A (contact switch)	peak: 10 mW (motor) 313 W (contact switch)	peak: 13.23 W m^{-3} (motor, core device)	rectangular inner part: 12 cm × 9 cm	PTFE, soft membrane, Al, Cu	contact separation	2017	high output
spring-assisted spherical TENG [38]	multilayer, mass-spring	0.67 μC	120 μA	peak: 7.96 mW	peak: 15.2 W m^{-3}	sphere diameter 10 cm	Kapton, FEP, spring, Cu, Al	contact separation	2018	
nodding duck structure multi-track TENG [39] (NDM-FTENG)	multilayer, rolling		~1.1 μA (two devices, wave)		peak: 4 W m^{-3} (motor, 0.21 Hz)	10 cm × 20 cm (width by height)	PPCF (PVDF/PDMS composite films), nylon, Cu, PET, PMMA	freestanding	2021	
tandem disk TENG [27] (TD-TENG)	grating, pendulum, multilayer	3.3 μC (wave, 0.58 Hz)		peak: 45.0 mW (wave, 0.58 Hz) average: 7.5 mW (wave, 0.58 Hz)	peak: 7.89 W m^{-3} (wave, 0.58 Hz) average: 1.3 W m^{-3} (wave, 0.58 Hz) 7.3 W m^{-3} (wave, 0.58 Hz, core device)	volume 0.0057 m^3	PTFE, acrylic, Cu	freestanding	2019	high power density
single pendulum inspired TENG (P-TENG) [22]	pendulum, spacing	18.2 nC (motor, 0.017 Hz)				sphere diameter 13 cm	PTFE, Cu, acrylic, cotton thread	freestanding	2019	durable
robust swing-structured TENG [40] (SS TENG)	pendulum, spacing	256 nC (wave, 1.2 Hz)	5.9 μA (wave, 1.2 Hz)	peak: 4.56 mW (motor, 0.017 Hz)	peak: 1.29 W m^{-3} (motor, 0.017 Hz)	cylindrical shell: length 20 cm, outer diameter 15 cm	PTFE, Cu, acrylic	freestanding	2020	durable

Device	Feature	Typical Output				Dimension Per Unit	Material	Mode	Year	Note
		Q_{sc}	I_{sc}	Power	Power Density					
active resonance TENG [41] (AR-TENG)	pendulum, multilayer	0.55 μC (wave)	120 μA (wave)	peak: 12.3 mW (wave)	peak: 16.31 W m^{-3} (wave, core device)	volume 754 cm^3 (core device)	FEP, Kapton, Cu	contact separation	2021	omnidirectior
spiral TENG [42]	mass-spring		15 μA (wave)		peak: 2.76 W m^{-2} (motor, 30 Hz)	sphere diameter 14 cm	Kapton, Cu, Al	contact separation	2013	
liquid solid electrification enabled generator [32] (LSEG)	L-S contact	75 nC (motor, 0.5 m/s)	3 μA (motor, 0.5 m/s)	average: 0.12 mW (motor, 0.5 m/s)	average: 0.067 W m^{-2} (motor, 0.5 m/s)	planar: 6 cm × 3 cm	water, FEP, Cu	freestanding	2014	
networked integrated TENG [43] (NI-TENG)	L-S contact		13.5 μA (motor, 0.5 m/s)	peak: 1.03 mW (motor, 0.5 m/s)	peak: 0.147 W m^{-2} (motor, 0.5 m/s)	planar: 10 cm × 7 cm	Kapton, PTFE, water	freestanding	2018	
TENG based on charge shuttling [33] (CS-TENG)	charge pumping, multilayer	53 μC (rectified, wave, 0.625 Hz)	1.3 mA (wave, 0.625 Hz)	peak: 126.67 mW (wave, 0.625 Hz)	peak: 30.24 W m^{-3} (wave, 0.625 Hz)	sphere diameter 20 cm	PTFE, PP, Cu, Zn-Al	contact separation	2020	high charge output

(2) The durability of the TENG with friction or contact interfaces should be further examined and optimized. For long-term operation at sea, the device should achieve high reliability.

(3) The networking strategy is important for organizing and coupling TENG units together to reach higher efficiency as an integrated system. It is less investigated in the past for its complexity, which should be emphasized with further development of blue energy.

(4) The interaction of devices with water motion is crucial for power-take-off (PTO) performance of the system, which should be theoretically investigated and optimized based on fluid-structure interaction dynamics.

(5) Adaptability to the ocean environment involves packaging of the device, antifouling, and anticorrosion, which can ensure that the function of the network is not damaged in the severe ocean environment. The complete encapsulation of the device by waterproof materials can protect the circuit and core device from water.

(6) Hybrid harvesting that can harness various other energy forms at sea, such as wind, rain drops, and sun light, can further improve the utilization efficiency of certain ocean area [44].

(7) Environmentally friendly designs and degradable materials are also highly required to reduce the environment risks of such systems in ocean [45].

(8) Power management that optimizes at the module level or network level is highly required, which extends the present work to larger systems. It is expected to greatly improve the total efficiency of the whole system.

References

1. Isaacs, J.D.; Schmitt, W.R. Ocean Energy: Forms and Prospects. Science 1980, 207, 265.
2. Salter, S.H. Wave power. Nature 1974, 249, 720–724.
3. Ellabban, O.; Abu-Rub, H.; Blaabjerg, F. Renewable energy resources: Current status, future prospects and their enabling technology. Renew. Sust. Energ. Rev. 2014, 39, 748–764.
4. Marshall, B.; Ezekiel, C.; Gichuki, J.; Mkumbo, O.; Sitoki, L.; Wanda, F. Global warming is reducing thermal stability and mitigating the effects of eutrophication in Lake Victoria (East Africa). Nat. Preced. 2009.

5. Barbarossa, V.; Bosmans, J.; Wanders, N.; King, H.; Bierkens, M.F.P.; Huijbregts, M.A.J.; Schipper, A.M. Threats of global warming to the world's freshwater fishes. Nat. Commun. 2021, 12, 1701.
6. Yamaguchi, M.; Chan, J.C.L.; Moon, I.-J.; Yoshida, K.; Mizuta, R. Global warming changes tropical cyclone translation speed. Nat. Commun. 2020, 11, 47.
7. van Soest, H.L.; den Elzen, M.G.J.; van Vuuren, D.P. Net-zero emission targets for major emitting countries consistent with the Paris Agreement. Nat. Commun. 2021, 12, 2140.
8. Tollefson, J. Power from the oceans: Blue energy. Nature 2014, 508, 302–304.
9. Qin, Y.; Alam, A.U.; Pan, S.; Howlader, M.M.R.; Ghosh, R.; Hu, N.-X.; Jin, H.; Dong, S.; Chen, C.-H.; Deen, M.J. Integrated water quality monitoring system with pH, free chlorine, and temperature sensors. Sens. Actuators B Chem. 2018, 255, 781–790.
10. Callaway, E. Energy: To catch a wave. Nature 2007, 450, 156–159.
11. Xi, F.; Pang, Y.; Liu, G.; Wang, S.; Li, W.; Zhang, C.; Wang, Z.L. Self-powered intelligent buoy system by water wave energy for sustainable and autonomous wireless sensing and data transmission. Nano Energy 2019, 61, 1–9.
12. Khaligh, A.; Onar, O.C. Energy Harvesting—Solar, Wind, and Ocean Energy Conversion Systems; CRC: Boca Raton, FL, USA, 2009; Volume 89.
13. Chu, S.; Majumdar, A. Opportunities and challenges for a sustainable energy future. Nature 2012, 488, 294–303.
14. Wang, Z.L. Entropy theory of distributed energy for internet of things. Nano Energy 2019, 58, 669–672.
15. Niu, S.; Wang, Z.L. Theoretical systems of triboelectric nanogenerators. Nano Energy 2015, 14, 161–192.
16. Niu, S.; Wang, S.; Lin, L.; Liu, Y.; Zhou, Y.S.; Hu, Y.; Wang, Z.L. Theoretical study of contact-mode triboelectric nanogenerators as an effective power source. Energy Environ. Sci. 2013, 6, 3576–3583.
17. Niu, S.; Liu, Y.; Wang, S.; Lin, L.; Zhou, Y.S.; Hu, Y.; Wang, Z.L. Theory of Sliding-Mode Triboelectric Nanogenerators. Adv. Mater. 2013, 25, 6184–6193.
18. Niu, S.; Liu, Y.; Wang, S.; Lin, L.; Zhou, Y.S.; Hu, Y.; Wang, Z.L. Theoretical Investigation and Structural Optimization of Single-Electrode Triboelectric Nanogenerators. Adv. Funct. Mater. 2014, 24, 3332–3340.
19. Niu, S.; Liu, Y.; Chen, X.; Wang, S.; Zhou, Y.S.; Lin, L.; Xie, Y.; Wang, Z.L. Theory of freestanding triboelectric-layer-based nanogenerators. Nano Energy 2015, 12, 760–774.
20. Wang, Z.L. Catch wave power in floating nets. Nature 2017, 542, 159–160.
21. Wang, Z.L. From contact-electrification to triboelectric nanogenerators. Rep. Prog. Phys. 2021.
22. Lin, Z.; Zhang, B.; Guo, H.; Wu, Z.; Zou, H.; Yang, J.; Wang, Z.L. Super-robust and frequency-multiplied triboelectric nanogenerator for efficient harvesting water and wind energy. Nano Energy 2019, 64, 103908.
23. Yang, X.; Xu, L.; Lin, P.; Zhong, W.; Bai, Y.; Luo, J.; Chen, J.; Wang, Z.L. Macroscopic self-assembly network of encapsulated high-performance triboelectric nanogenerators for water wave energy harvesting. Nano Energy 2019, 60, 404–412.
24. Xu, L.; Pang, Y.; Zhang, C.; Jiang, T.; Chen, X.; Luo, J.; Tang, W.; Cao, X.; Wang, Z.L. Integrated triboelectric nanogenerator array based on air-driven membrane structures for water wave energy harvesting. Nano Energy 2017, 31, 351–358.
25. Zhao, X.J.; Zhu, G.; Fan, Y.J.; Li, H.Y.; Wang, Z.L. Triboelectric Charging at the Nanostructured Solid/Liquid Interface for Area-Scalable Wave Energy Conversion and Its Use in Corrosion Protection. ACS Nano 2015, 9, 7671–7677.
26. Xu, L.; Bu, T.Z.; Yang, X.D.; Zhang, C.; Wang, Z.L. Ultrahigh charge density realized by charge pumping at ambient conditions for triboelectric nanogenerators. Nano Energy 2018, 49, 625–633.
27. Bai, Y.; Xu, L.; He, C.; Zhu, L.; Yang, X.; Jiang, T.; Nie, J.; Zhong, W.; Wang, Z.L. High-performance triboelectric nanogenerators for self-powered, in-situ and real-time water quality mapping. Nano Energy 2019, 66, 104117.
28. Kim, D.Y.; Kim, H.S.; Kong, D.S.; Choi, M.; Kim, H.B.; Lee, J.-H.; Murillo, G.; Lee, M.; Kim, S.S.; Jung, J.H. Floating buoy-based triboelectric nanogenerator for an effective vibrational energy harvesting from irregular and random water waves in wild sea. Nano Energy 2018, 45, 247–254.
29. Liu, G.; Xiao, L.; Chen, C.; Liu, W.; Pu, X.; Wu, Z.; Hu, C.; Wang, Z.L. Power cables for triboelectric nanogenerator networks for large-scale blue energy harvesting. Nano Energy 2020, 75, 104975.
30. Xi, F.; Pang, Y.; Li, W.; Jiang, T.; Zhang, L.; Guo, T.; Liu, G.; Zhang, C.; Wang, Z.L. Universal power management strategy for triboelectric nanogenerator. Nano Energy 2017, 37, 168–176.
31. Liu, W.; Wang, Z.; Wang, G.; Zeng, Q.; He, W.; Liu, L.; Wang, X.; Xi, Y.; Guo, H.; Hu, C.; et al. Switched-capacitor-convertors based on fractal design for output power management of triboelectric nanogenerator. Nat. Commun. 2020, 11, 1883.

32. Zhu, G.; Su, Y.; Bai, P.; Chen, J.; Jing, Q.; Yang, W.; Wang, Z.L. Harvesting Water Wave Energy by Asymmetric Screening of Electrostatic Charges on a Nanostructured Hydrophobic Thin-Film Surface. ACS Nano 2014, 8, 6031–6037.
33. Wang, H.; Xu, L.; Bai, Y.; Wang, Z.L. Pumping up the charge density of a triboelectric nanogenerator by charge-shuttling. Nat. Commun. 2020, 11, 4203.
34. Liu, Y.; Liu, W.; Wang, Z.; He, W.; Tang, Q.; Xi, Y.; Wang, X.; Guo, H.; Hu, C. Quantifying contact status and the air-breakdown model of charge-excitation triboelectric nanogenerators to maximize charge density. Nat. Commun. 2020, 11, 1599.
35. Yu, Y.; Li, Z.; Wang, Y.; Gong, S.; Wang, X. Sequential Infiltration Synthesis of Doped Polymer Films with Tunable Electrical Properties for Efficient Triboelectric Nanogenerator Development. Adv. Mater. 2015, 27, 4938–4944.
36. Wang, X.; Niu, S.; Yin, Y.; Yi, F.; You, Z.; Wang, Z.L. Triboelectric Nanogenerator Based on Fully Enclosed Rolling Spherical Structure for Harvesting Low-Frequency Water Wave Energy. Adv. Energy Mater. 2015, 5, 1501467.
37. Xu, L.; Jiang, T.; Lin, P.; Shao, J.J.; He, C.; Zhong, W.; Chen, X.Y.; Wang, Z.L. Coupled Triboelectric Nanogenerator Networks for Efficient Water Wave Energy Harvesting. ACS Nano 2018, 12, 1849–1858.
38. Xiao, T.X.; Liang, X.; Jiang, T.; Xu, L.; Shao, J.J.; Nie, J.H.; Bai, Y.; Zhong, W.; Wang, Z.L. Spherical Triboelectric Nanogenerators Based on Spring-Assisted Multilayered Structure for Efficient Water Wave Energy Harvesting. Adv. Funct. Mater. 2018, 28, 1802634.
39. Liu, L.; Yang, X.; Zhao, L.; Hong, H.; Cui, H.; Duan, J.; Yang, Q.; Tang, Q. Nodding Duck Structure Multi-track Directional Freestanding Triboelectric Nanogenerator toward Low-Frequency Ocean Wave Energy Harvesting. ACS Nano 2021, 15, 9412–9421.
40. Jiang, T.; Pang, H.; An, J.; Lu, P.; Feng, Y.; Liang, X.; Zhong, W.; Wang, Z.L. Robust Swing-Structured Triboelectric Nanogenerator for Efficient Blue Energy Harvesting. Adv. Energy Mater. 2020, 10, 2000064.
41. Zhang, C.; He, L.; Zhou, L.; Yang, O.; Yuan, W.; Wei, X.; Liu, Y.; Lu, L.; Wang, J.; Wang, Z.L. Active resonance triboelectric nanogenerator for harvesting omnidirectional water-wave energy. Joule 2021, 5, 1613–1623.
42. Hu, Y.; Yang, J.; Jing, Q.; Niu, S.; Wu, W.; Wang, Z.L. Triboelectric Nanogenerator Built on Suspended 3D Spiral Structure as Vibration and Positioning Sensor and Wave Energy Harvester. ACS Nano 2013, 7, 10424–10432.
43. Zhao, X.J.; Kuang, S.Y.; Wang, Z.L.; Zhu, G. Highly Adaptive Solid–Liquid Interfacing Triboelectric Nanogenerator for Harvesting Diverse Water Wave Energy. ACS Nano 2018, 12, 4280–4285.
44. Xu, L.; Xu, L.; Luo, J.; Yan, Y.; Jia, B.-E.; Yang, X.; Gao, Y.; Wang, Z.L. Hybrid All-in-One Power Source Based on High-Performance Spherical Triboelectric Nanogenerators for Harvesting Environmental Energy. Adv. Energy Mater. 2020, 10, 2001669.
45. Chen, G.; Xu, L.; Zhang, P.; Chen, B.; Wang, G.; Ji, J.; Pu, X.; Wang, Z.L. Seawater Degradable Triboelectric Nanogenerators for Blue Energy. Adv. Mater. Technol. 2020, 5, 2000455.